

BEAM TEST OF A FRONT-END SYSTEM FOR THE JAERI-KEK JOINT (JKJ) PROJECT

A. Ueno, K. Ikegami, M. Okada, S. Arai, E. Kadokura, S. Noguchi, Z. Igarashi, C. Kubota,
N. Kamikubota, M. Ikegami, K. Yoshino, Y. Fukui, M. Kawamura, S. Yamaguchi, S. Fukuda,
S. Anami, KEK, Tsukuba 305-0801, Japan
Y. Kondo, H. Oguri, JAERI, Tokai 319-1195, Japan

Abstract

Beam characteristics of a front-end system of the JKJ linac was measured. The measured transverse emittance of a 27mA beam extracted from the negative hydrogen ion source (NIS) was within the assumed range in RFQ design. The measured transmission of the RFQ showed a good agreement with PARMTEQm[1] simulation. Significant emittance growth was observed in the medium energy beam transport (MEBT) following the RFQ. In order to reproduce the Twiss parameter measured at the MEBT exit in TRACE3D[2] calculation, input data representing the realistic field distribution in each quadrupole(Q) magnet was indispensable.

1 INTRODUCTION

A front-end system, which is composed of a NIS, a low energy beam transport (LEBT) with two short strong-field solenoid magnets (SMAG's) and a 324MHz radio frequency quadrupole (RFQ) linac, was originally developed for the Japan Hadron Facility (JHF) project [3,4,5]. According to the requirement of the JHF, the RFQ was designed to accelerate 30mA beam with a transmission of more than 90% while minimizing the accelerated beam emittances. The challenging goal of a intensity of more than 33mA with a duty factor of more than 1.5% (600micro-sec*25Hz) for the "cesium unseeded" NIS was settled in order to avoid the instability due to sparking in the extraction and acceleration gaps of the NIS and the inter-vane gaps of the RFQ caused by introduced cesium. The front-end system is operated in order to supply a beam for testing downstream parts of the JKJ linac. The results of beam test are described.

2 EXPERIMENTAL SETUP

A schematics of the NIS and LEBT is shown in Fig.1a). A LaB₆ filament was used to produce DC-arc plasma in the NIS. The beam extracted from the NIS was injected into the RFQ being focused with two SMAG's. The beam current was measured with a movable Faraday-cup (FCm). The horizontal and vertical emittances of the beam were measured with two sets of double slit type emittance monitor composed of a movable slit (EMSL) and a movable Faraday-cup with slit (EMFC). FCm, EMSL and EMFC were installed on a vacuum chamber located between two SMAG's.

A schematics of a set-up to measure the beam just after the RFQ is shown in Fig.1b). Emittances of the RFQ beam were measured with two sets of double slit type

emittance monitor as same as on the LEBT. The beam current was measured with a current transformer (CT1) and a Faraday-cup (FC). During the measurements, the beam was focused with two Q-magnets (Q1 and Qtst).

A schematics of a set-up to measure the beam after the MEBT is shown in Fig.1c). The beam current was measured with CT1, CT2 and FC. The emittances were also measured in this set-up.

3 RESULTS OF THE BEAM TEST

As shown by trace1 of Fig.2, the NIS produced a peak beam current of 27mA. In order to chop macro beam pulse by using the longitudinal acceptance of the RFQ, the acceleration voltage of the NIS was modulated from 33kV to 42kV with a rising time of a few μ s at 180 μ s later from trigger. The measured current increased with a slight step at the same timing. The beam energy became the design value of 50keV, when the acceleration voltage was 42kV, since the extraction voltage was set to 8kV. The pulse arc power was calculated to be 50kW from trace2 and 3 ($I_{arc}=240A$ and $V_{arc}=210V$).

As shown by trace1 of Fig.3, macro beam pulse after the RFQ was chopped with a few μ s rising time by modulating acceleration voltage of the NIS and around 1 μ s falling time by offing the rf-switch of rf-source for the RFQ. The accelerated beam current was 25mA.

For a 10mA beam, horizontal and vertical emittances were measured with set-up shown in Fig.1b). The Twiss parameter trace-backed with TRACE3D at the exit of the RFQ is shown in Fig.4a). PARMTEQm simulation results for 10mA and 25mA beams are shown in Fig.4a) and b). Although the simulated Twiss parameters are similar for two different currents ($\alpha_x, \beta_x, \alpha_y, \beta_y=-1.85, 0.16, 1.53, 0.13$ for 10mA and $-1.95, 0.17, 1.56, 0.13$ for 25mA), the measured one ($\alpha_x, \beta_x, \alpha_y, \beta_y=-1.22, 0.13, 2.19, 0.22$) is rather discrepant with them. The vane-end round cutting (to resist high voltage sparking) not included in the simulation probably caused the discrepancy.

The particle distribution in the horizontal/vertical phase space (top) and the relationship between the emittance and the beam fraction included in it (bottom) measured with set-up shown in Fig.1c) is shown in Fig.5/6. The measured normalized rms emittances in different conditions are listed in Table 1. RFQ1 and 2 of Table 1 are according to datum shown in Fig.4a) and Fig.5, respectively. A significant emittance growth (5%/12% in horizontal/vertical phase space) was caused by changing only coil current of Q8 slightly (comparison between

RFQ2 and 3). In both cases (RFQ2 and 3), although the emittance in horizontal phase space was grown more than 25% (comparison with IS2), the emittance in vertical phase space was conserved as simulated result (comparison between IS2 and RFQ2).

As shown in Fig.7, the emittances shown in Fig.5 and 6 was compared with TRACE3D calculation using the measured Twiss parameter of Fig.2a) as initial condition for two different cases of 60mm Q-field length(a) or 80mm(b). In both cases, the GL (field gradient times length) was set to the integrated value of field distribution calculated with MAFIA, Twiss parameter was rather discrepant with the measurement. Since the bore diameter of each Q-magnet is comparable with it's length as shown in Table 2, each Q-magnet produces rather large fringe field as MAFIA [6] calculations shown in Fig.8(top). By composing each Q-magnet with 20 components, each of which has one of the field gradient shown in Fig.8(bottom), TRACE3D calculation showed a good agreement with the measurement as shown in Fig.9. Since the length of each component is 10mm, the total length of each Q-field is 200mm.

4 CONCLUSIONS

The cesium unseeded NIS produced a 27mA negative hydrogen beam with a low duty factor of 0.1% (100μs*12.5Hz). The measured transverse emittance ($\epsilon_{x/y\text{rms}}=0.2\pi\text{mm}^*\text{mrad}$) of the beam was within the two assumed values(0.167 and 0.25πmm*mrad) used in RFQ design. The measured transmission (93%) of the RFQ showed a good agreement with PARMTEQM simulation. However, the measured Twiss parameter at the RFQ exit was discrepant with the simulation, probably due to the

effect of round cutting of vane-end. Significant emittance growth (upto 30% in rms value) in the MEBT was observed. Although the causes of the growth are not specified, horizontal emittance measured at LEBT was conserved at the MEBT exit in one MEBT setting. A MEBT setting, which minimize emittance growth in both phase spaces will be studied. By composing each Q-magnet in MEBT with 20 components representing the realistic field distribution, TRACE3D reproduced the measurements.

5 REFERENCES

- [1] K. R. Crandall et al., RFQ Design Codes, LA-UR-96-1836, revised Aug. 1998.
- [2] K. R. Crandall and D. P. Rusthoi, TRACE3D Documentation, LA-UR-97-886, May 1997.
- [3] JHF Project Office, KEK Report 97-16, 4.4, (1998).
- [4] A. Ueno et al., SLAC-R-561, 256, (2000).
- [5] A. Ueno and Y. Kondo, SLAC-R-561, 545, (2000).
- [6] T. Weiland, Part. Accel., 17, 227, (1985).

Table 1: Measured Normalized Emittance (πmm*mrad)

	$I_{\text{beam}}(\text{mA})$	ϵ_{nrmsx}	ϵ_{nrmsy}
IS1: At RFQ Entrance	8	0.107	0.101
IS2: Between two SMAGs	27	0.200	0.202
RFQ1: After Qtst	10	0.173	0.194
RFQ2: After Q8($I_{Q8}=28\text{A}$)	25	0.250	0.201
RFQ3: After Q8($I_{Q8}=55\text{A}$)	25	0.262	0.226

Table 2: Parameter of Quadrupole Magnets

	Q1	Qtst	Q2/3/6/7/8	Q4/5
Core Length (mm)	60	50	60	60
Bore Diameter (mm)	30	35	41	52
Coil Turns per Pole	15	17	19	19

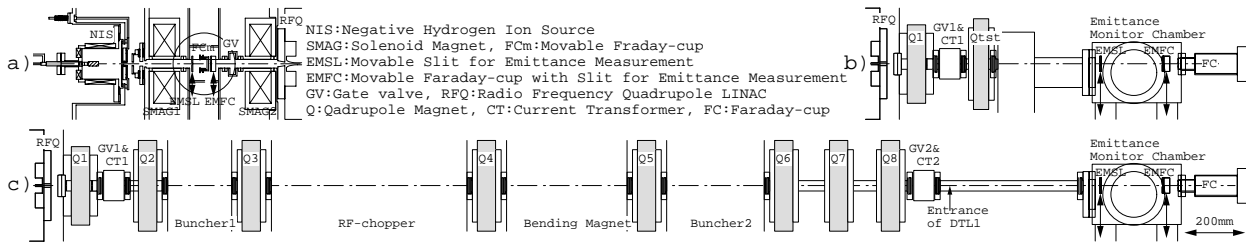


Figure 1: a) Schematics of the NIS and LEBT. b) Schematics of set-up to measure the beam just after the RFQ. C) Schematics of MEBT and set-up to measure the beam transported through the MEBT.

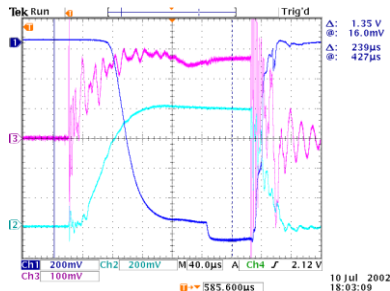


Figure 2: Waveforms of beam current measured with FCm on LEBT (tracel: 4mA/Div.), arc current (trace2: 60A/Div.) and arc voltage (trace3: 80V/Div.). Repetition rate of pulses was 12.5Hz. Time scale is 40μs/Div..

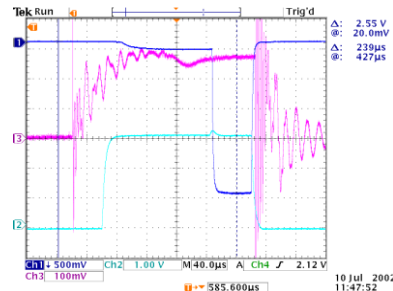


Figure 3: Waveforms of beam current measured with CT1 on MEBT (tracel: 5mA/Div.), RFQ tank filed (trace2). Repetition rates of NIS and RFQ pulses were 12.5Hz and 25Hz, respectively. Time scale is 40μs/Div..

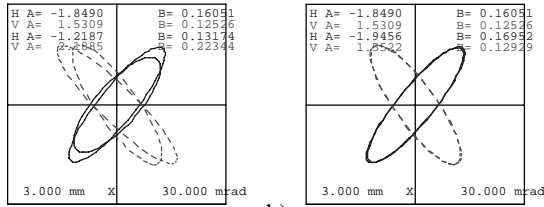


Figure 4: a) Measured and simulated Twiss parameters at the exit of the RFQ for a 10mA beam. b) The simulated Twiss parameters for 10mA and 25mA beams.

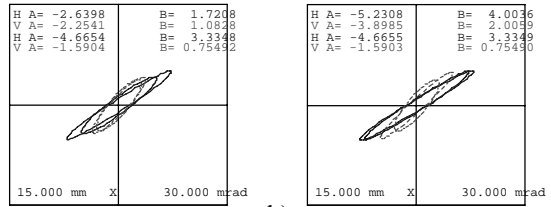


Figure 7: Measured and traced Twiss parameters at emittance monitor position of Fig.1c). Q-field length used in TRACE3D was 60mm(a) and 80mm(b).

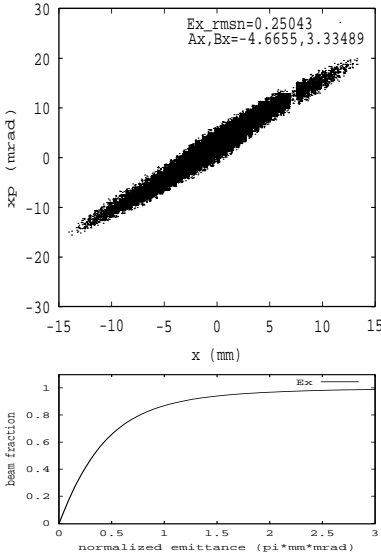


Figure 5: Measured particle distribution in horizontal phase space (top) and relationship between emittance and beam fraction included in emittance (bottom).

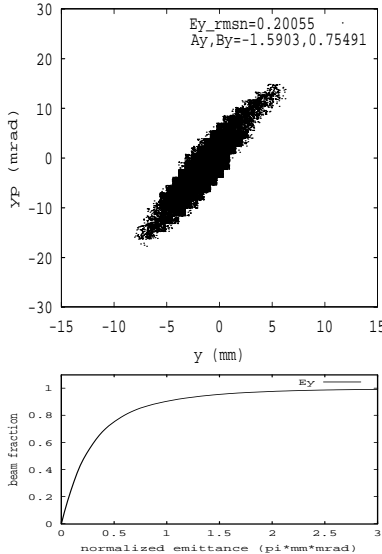


Figure 6: Measured particle distribution in vertical phase space (top) and relationship between emittance and beam fraction included in emittance (bottom).

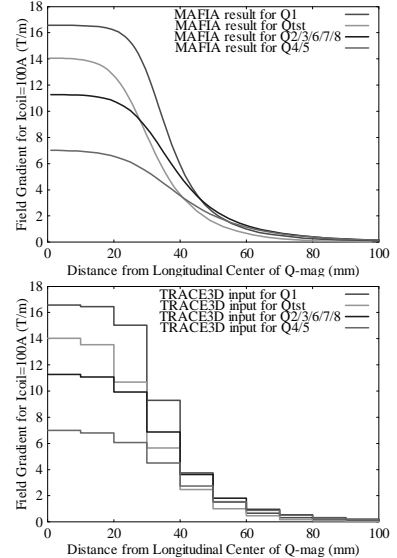


Figure 8: Field gradient distributions in four type of Q-magnets for coil current of 100A calculated with MAFIA (top) and used in TRACE3D calculations (bottom).

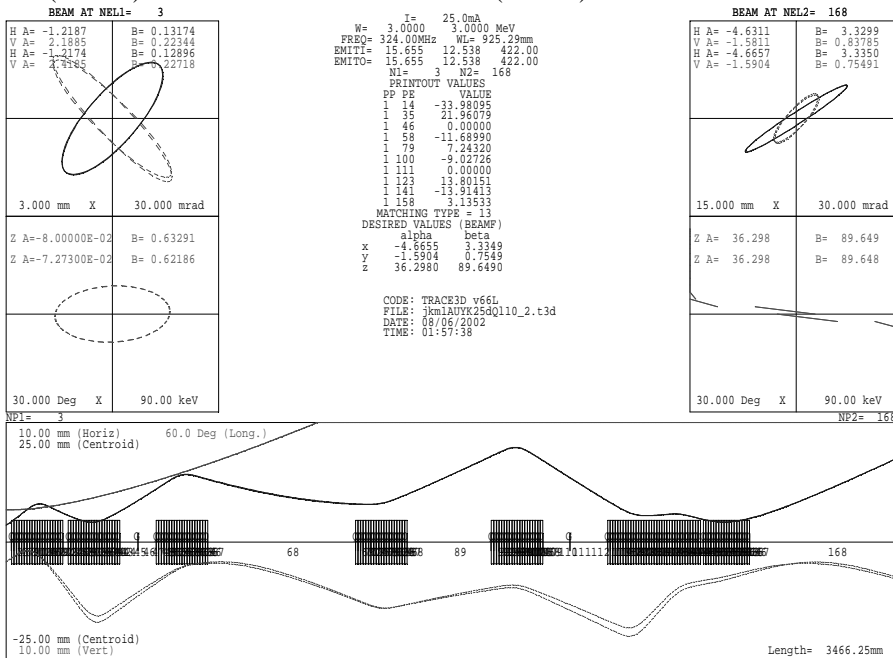


Figure 9: TRACE3D results using realistic filed distribution in each quadrupole magnet. Traced orbit using Twiss parameter estimated from the emittances measured with set-up shown in Fig.1b) and trace-backed orbit using the emittances measured with set-up shown in Fig.1c) are presented. ($I_{Q1/2/3/4/5/6/7/8}=205/195/104/104/129/123/124/28A$)